Simulation of flow over double-element airfoil and wind tunnel test for use in vertical axis wind turbine

2014 J. Phys.: Conf. Ser. 524 012009

(http://iopscience.iop.org/1742-6596/524/1/012009)

Simulation of flow over double-element airfoil and wind tunnel test for use in vertical axis wind turbine

Prasad Chougule
Søren R.K. Nielsen

Department of civil Engineering, Aalborg University, Sohngaardsholmsvej 57, 9000-Aalborg, Denmark.

E-mail: pdc@civil.aau.dk; Ph. No. +45 5261 7115

Abstract. Nowadays, small vertical axis wind turbines are receiving more attention due to their suitability in micro-electricity generation. There are few vertical axis wind turbine designs with good power curve. However, the efficiency of power extraction has not been improved. Therefore, an attempt has been made to utilize high lift technology for vertical axis wind turbines in order to improve power efficiency. High lift is obtained by double-element airfoil mainly used in aeroplane wing design. In this current work a low Reynolds number airfoil is selected to design a double-element airfoil blade for use in vertical axis wind turbine to improve the power efficiency. Double-element airfoil blade design consists of a main airfoil and a slat airfoil. Orientation of slat airfoil is a parameter of investigation in this paper and air flow simulation over double-element airfoil. With primary wind tunnel test an orientation parameter for the slat airfoil is initially obtained. Further a computational fluid dynamics (CFD) has been used to obtain the aerodynamic characteristics of double-element airfoil. The CFD simulations were carried out using ANSYS CFX software. It is observed that there is an increase in the lift coefficient by 26% for single-element airfoil at analysed conditions. The CFD simulation results were validated with wind tunnel tests. It is also observe that by selecting proper airfoil configuration and blade sizes an increase in lift coefficient can further be achieved.

1. Introduction

Various types of vertical-axis wind turbines (VAWTs) have been suggested. The most well-known include the Darrieus-type egg beater-shaped VAWT invented in 1931 [1], the Savonius type VAWT invented in 1929, and the H-rotor type design, which appeared after research activity from 1970 to 1980 in the UK. Darrieus VAWTs have recently been documented as an alternative solution for small power production [2]-[3]. Eriksson et al. concluded that VAWTs are more cost-effective than horizontal axis wind turbines (HAWTs) for small power generation [4]. A Darrieus-type VAWT consists of three blades with straight, curved, spiral, helical geometry to improve their power coefficient. In this paper straight bladed VAWT is consider because author wanted to implement self active pitch control mechanism [5].

Bhutta et al. [6] summarized the designs and techniques of VAWTs and compared their performances. VAWTs that operate by a lift force are conventionally designed using a single airfoil in the blade design. There are two main types of airfoils: symmetric and non-symmetric. Symmetric airfoils were developed by the National Advisory Committee of Aeronautics (NACA) for use in low-altitude-flying airplanes. A conventional straight-bladed VAWT design has two

essential drawbacks: i) it shows low power coefficient compared to the horizontal-axis wind turbine (HAWT), and ii) it does not start itself. In this paper, the power coefficient of a conventional VAWT was improved by using a double-element airfoil in the blade design. The operating principle of the multi-element airfoil has been nicely represented by Smith [7]. The purpose of a multi-element airfoil is to increase the lift coefficient and delay the stall angle of a single airfoil [8],[9]. The lift coefficient is directly proportional to the mechanical power output. Therefore, an increase in the lift coefficient of a double-element airfoil should improve the power coefficient of VAWT.

Gaunaa et al. previously tried to determine the aerodynamic characteristics of a double-element airfoil, emphasizing its applicability in the HAWT [10]. They studied the double-element airfoil for high Reynolds numbers of magnitude $Re \geq 1,000,000$. A computational fluid dynamic (CFD) simulation of the flow around a double-element airfoil showed a remarkable increase in lift coefficient. However, VAWT operates at very low range of Reynolds numbers ($Re = 100,000 - 300,000$). The condition of very low Reynolds number was the most critical part in the flow physics over the airfoil, because the flow behavior was drastically different compared to other conditions and standard flow theories might predict the wrong results. Therefore, care was taken during meshing and a selection of an airfoil providing a high lift coefficient at low Reynolds number.

The size of the slat airfoil with respect to the main airfoil was decided based on the design guidelines given by Buhl [11]. The position and optimal angle of the slat airfoil with respect to the main airfoil were determined by a wind-tunnel experiment, to achieve the maximum lift coefficient. 2D CFD simulation of double-element airfoil is performed in this study and aerodynamic characteristics of the slat airfoil and main airfoil are discussed. A sample test of validation was carried out to compare the 2D CFD over all results with the wind tunnel test.

Section 2 discusses the selection and design of the double-element airfoil. Section 3 gives the wind tunnel experiment carried out with double-element airfoil. Section 4 discusses detail about the 2D CFD modeling and simulation and a sample validation is given. Section 5 contains the conclusion part of the study.

2. Airfoil configuration

A common practice in the design of an airfoil for a VAWT is to modify available NACA symmetric airfoils. These airfoils were designed for low-altitude airplanes, for which the flow conditions nearly correspond to the flow physics around the VAWT. However, these airfoils are not the optimal choice for blade design in VAWTs that operate at low Reynolds numbers. Airfoils that perform well at low Reynolds numbers are more suitable. In this context , the S1210 and S1223 airfoils have proven to be better than the symmetric or non-symmetric NACA airfoils [12]. They were originally designed to obtain high lift at high altitude for a drone, characteristics that can be used in VAWT blade design.

2.1. Airfoil Selection

The airfoil shape contributes in the generation of a lift coefficient by creating suction on upper surface of the airfoil. In this process, a drag is also being generated which is not desirable for the maximum power output of the wind turbine. To get the maximum torque and a power output from wind turbine, it is important to have an airfoil which will generate the high-lift and the high lift-to-drag ratio. Selection of a proper airfoil for the VAWT is very important at initial stage of the design process. In [13] it is summarized that the operating range for a symmetric airfoil is wider than the non-symmetric airfoil. That means that stall is observed at smaller angle of attack in case of a non-symmetric airfoil.

An airfoil designed at Delft University of Technology, Netherlands called the DU06-W200 has shown improvement in the lift coefficient and ability to self- start at low Reynolds number, [14].

An addition of a camber in the airfoil shape has contributed in a self start ability. The thickness of the base airfoil is increased to give more structural strength to the blades; however, it has not been justified with its need for the VAWT. In reality, the thick airfoil has the disadvantages of lowering the maximum lift coefficient even though it works at higher tip speed ratio. The increase in the power coefficient achieved up to 5% as compared to the use of the NACA0018 airfoil in a VAWT blade design.

There are a few other airfoils which operate at the low Reynolds number, mainly they are S1210, S1213 [15] and S1223 [16], [12]. These airfoils have the high-lift at a low Reynolds number from $Re = 200,000$ to $Re = 500,000$. Recently, a new airfoil for a small horizontal axis wind turbine has been designed by focusing a low wind speed startup which is called *airfish* AF300 [17]. The author has mentioned that, this airfoil works for Reynolds number ranging from $Re = 38,000$ to $Re = 205,000$, which means, it is a very low wind speed condition. AF300 is designed by addition of 1% to 3% in the trailing edge of the airfoil S1223 and 1% to 5% thickness in trailing edge of the airfoil S1210.

In this paper, the focus is on the proper airfoil selection for double-element airfoil design. In [13] it is also indicated that an S1046 airfoil has highest power coefficient, so it is obvious to select this profile for the design. However, there is one thing to be considered which is that the Reynolds number at which this airfoil performs well is related to the tip speed ratio (TSR). Also, in the selection and design of the airfoil one must consider other parameters such as the airfoil lift-to-drag ratio (c_L/c_D) also known as glide ratio, endurance parameter, thickness, pitching moment, stall characteristics, and sensitivity to the roughness are all important factors, amongst others. Therefore, a S1210 airfoil has been studied due to the high-lift coefficient at a low Reynolds number. The selection of a S1210 airfoil is done due to its maximum lift and higher lift-to-drag ratio. Further the design of double-element airfoil is carried out.

2.2. Double-element airfoil

In this paper, an S1210 airfoil was selected as the base airfoil for the design of a double-element airfoil. The S1210 airfoil has several characteristics that make it ideal for selection. i) It gives the highest maximum lift coefficient at a low Reynolds number. ii) It stalls smoothly; that is, the lift curve after the stall angle follows a nearly zero slope, represented by a glide ratio of (c_L/c_D). iii) It performs well at low Reynolds number and has the best combination of lift coefficient (c_L) and high glide ratio. c_L and c_D represents the lift and drag coefficients respectively.

The chord length c of the S1210 base airfoil was chosen to be c = 127 mm, based on the test specimen requirements of the Aerolab wind tunnel [18]. Figure 1 shows how the S1210 single airfoil was divided into a double-element airfoil (i.e., into a main airfoil and a slat airfoil). In the design of the double-element airfoil, the chord length of the slat airfoil (c_s) was 35% of

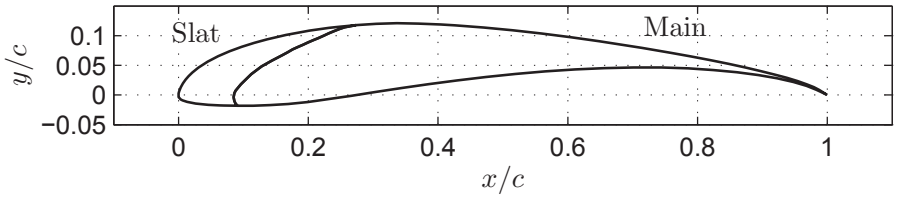

Figure 1. Division of a S1210 airfoil into a double-element airfoil

the chord length of the base airfoil c; thus, c_s (= 44.45 mm)[10],[11]. The main airfoil chord length (c_m) was 90% of c (= 114.3 mm). The design parameters of double-element airfoil, the position and slat angle with respect to the main airfoil are represented in the Figure 2. In the

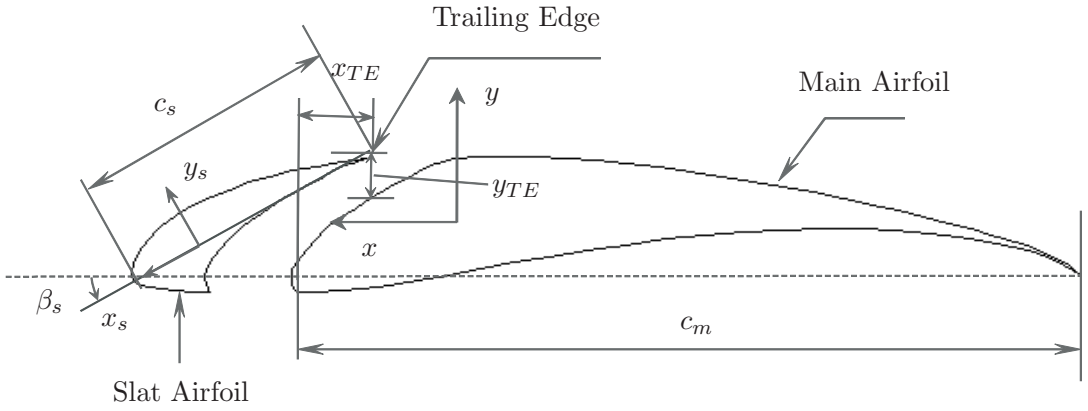

Figure 2. Double-element airfoil

double-element airfoil, the position and orientation of the slat airfoil with respect to the main airfoil are expressed by three parameters. Two parameters described the position of the trailing edge (TE) of a slat airfoil along the local $x-direction$ (x_{TE}) and the local $y-direction$ (y_{TE}). A third parameter, the slat angle (β_s), represented the orientation of the slat airfoil as the angle between the chord length of the slat airfoil with the local $x-direction$. This parameter is positive in the nose-up direction. In Table 1, TE corresponds with the trailing edge.

Table 1. Parameters of double-element airfoil

Description	Symbol	Value	Unit
Slat TE position x-direction	x_{TE}	0.012	m
Slat TE position y-direction	y_{TE}	0.004	m
Slat Aerofoil angle	β_s	-20	°

3. Wind tunnel experiment

A wind tunnel testing is performed in this work to:

- determine the optimal angle of a slat airfoil (β_s) with respect to the main airfoil.
- determine the lift and a drag coefficient of the double-element airfoil.
- validate the 2D CFD simulation results.

The dimensions of the wind tunnel used in this experiment are 305 mm width, 305 mm height and 610 mm length [18]. The range of the wind speed achievable is 4.5 m/s to 60 m/s. The wind tunnel used in this research has a limitation on the angle of attack which can be adjusted in the range of $-24°$ to $+24°$ due to the size of the wind tunnel. To avoid blockage effects the wind tunnel experiments are carried out at lower range of angle of attack $-20°$ to $+20°$. Also, it is important to mention here that the wind tunnel results are not influenced by blockage effect. Therefore, a 2D CFD simulation result obtained within this range of the angle of attack is compared with the wind tunnel test results.

The slat airfoil is bolted with a main airfoil by two side links fixed to the main airfoil, and a linear adjustment is provided by a slot on the link end so that, the position parameter x_{TE} can be adjusted. The y_{TE} position can be adjusted by rotating the links around main airfoil. The third parameter β_s is set by an angular position of a slat airfoil with respect to two side links parallel to the chord length of the main airfoil. The main and the slat airfoil blades are

manufactured by 3D printing technology, and plastic material is used. The optimum length of the double-element airfoil blade is 250 mm for this wind tunnel and is represented by h length of the double-element airfoil test blade.

The main and the slat airfoils are manufactured individually, and fixed to each other by side links as shown in Figure 3. Figure 3.a shows the top view of the double-element S1210 airfoil and Figure 3.b shows the bottom view of the double-element S1210 airfoil. A single airfoil is formed by joining a slat airfoil with the main airfoil and later used as a single airfoil test specimen in Aerolab wind tunnel. Then experiments are performed to find out the lift and the drag coefficients for a single and a double-element airfoil.

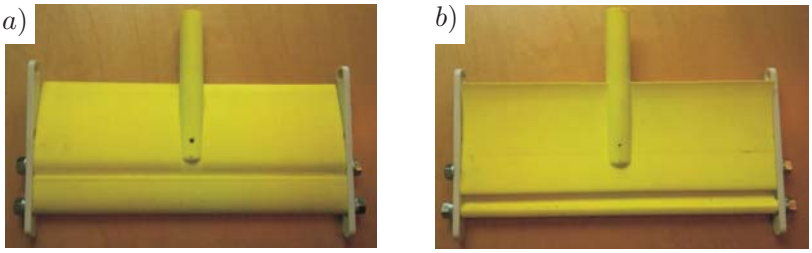

Figure 3. Double-element S1210 airfoil test specimen

The Aerolab wind tunnel has a data display and an acquisition system through which, the normal force N_f and the tangential force A_f acting on the double-element airfoil are obtained and stored in a text format. Theses forces are then converted to experimental lift force L_f and the drag force D_f by the following equation:

$$\left.\begin{aligned} L_f(\alpha) &= N_f\, cos(\alpha) - A_f\, sin(\alpha) \\ D_f(\alpha) &= N_f\, sin(\alpha) + A_f\, cos(\alpha) \end{aligned}\right\} \tag{1}$$

Finally, the experimental lift coefficient $c_{L_{expt}}$ and an experimental drag coefficients $c_{D_{expt}}$ are obtained:

$$\left.\begin{aligned} c_{L_{expt}} &= \frac{L_f}{\frac{1}{2}\,\rho V_m^2 (c_m + c_s)\, h} \\ c_{D_{expt}} &= \frac{D_f}{\frac{1}{2}\,\rho V_m^2 (c_m + c_s)\, h} \end{aligned}\right\} \tag{2}$$

Figure 4 shows the experimental lift coefficient of a single airfoil (SA) and a double-element airfoil (DA) for various Reynolds numbers.

At different Reynolds number, it is interesting to see that, the maximum lift coefficient for a single and double-element airfoil is increases, and also the stall angle is increased due to effect of the slat airfoil in front of the main airfoil. The effect of transition flow (laminar separation bubble)is occurred at $Re < 100,000$, therefore it is focused at $Re > 100,000$ in this paper. The tabular values represent the maximum lift coefficient for a single and double-element airfoil for different Reynolds number, and the difference in a stall angle is calculated and concluded with observations.

In Table 1, α_{max} represents the stall angle in the wind tunnel test. The difference of the stall angle between a single and double-element airfoil at $Re = 50,000$ is 11.2° which is very interesting, and it reduces to 8.6° for Re=100,000. From this it can be concluded that the S1210 double-element airfoil arrangement performs very well in the range of $Re = 50,000$ to $Re100,000$ by delaying the stall angle. Whereas, the difference of the maximum lift is gradually increasing

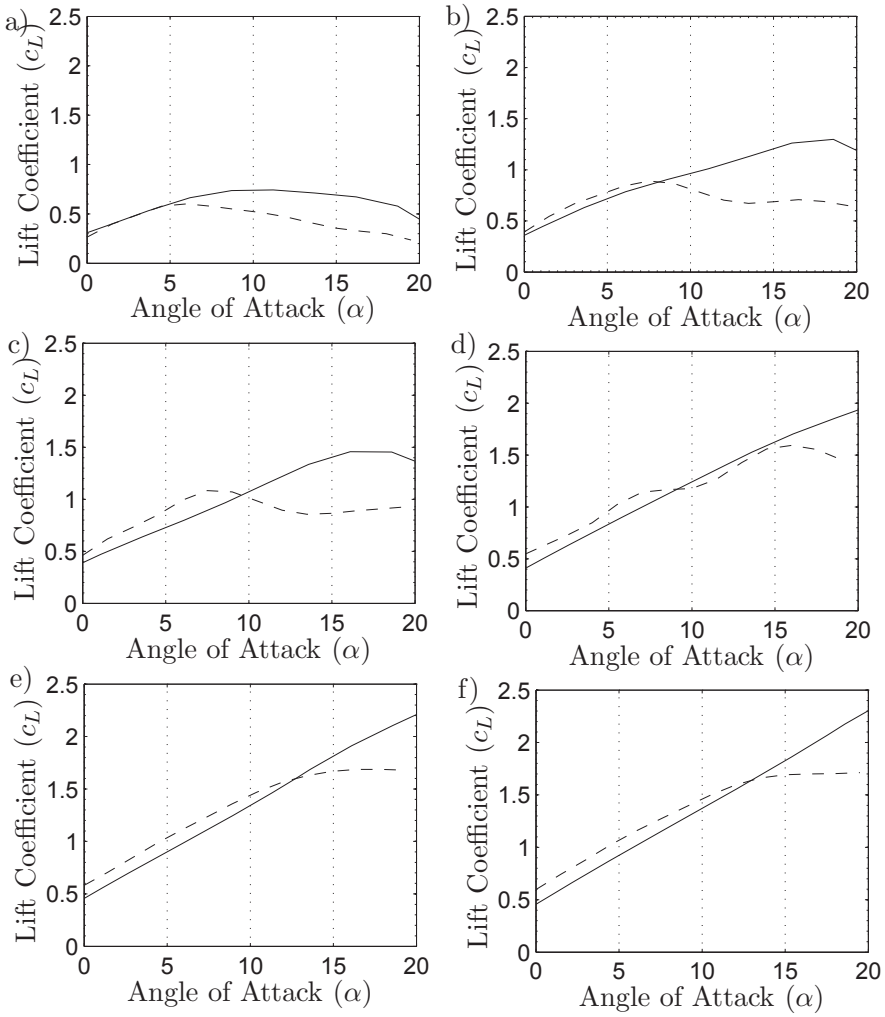

Figure 4. Wind Tunnel test results for Single and Double-element airfoils.
a) Re = 40,000 . b) Re = 55,000 . c) Re = 75,000. d) Re = 100,000. e) Re = 200,000. f) Re = 240,000
——: Double-element S1210 airfoil - - - -: Single-element S1210 airfoil

Table 2. The maximum experimental lift coefficient of a single (SA) and a double-element (DA) S1210 airfoil.

Re	$\alpha_{max}(SA)$	$c_{L_{max}}(SA)$	$\alpha_{max}(DA)$	$c_{L_{max}}(DA)$	$\Delta\alpha_{max}$	$\Delta c_{L_{max}}$
40,000	6°	0.6015	11.2°	0.7425	5.2°	0.1410
50,000	7.5°	0.8907	18.6°	1.257	11.2°	0.3663
75,000	7.5°	1.083	16.1°	1.457	8.6°	0.3740
100,000	16°	1.593	20°	1.935	—	—
200,000	16.4°	1.687	20°	2.200	—	—
240,000	19.5°	1.712	20°	2.310	—	—

which produces the extra power output. However, for the VAWT the delay of the stall angle improves the power efficiency more than the maximum lift coefficient. At the high wind speed conditions the effect of a slat airfoil on main airfoil has been less than in the low wind speed conditions. The S1210 airfoil has characteristics of the high lift coefficient at a low Reynolds number which supports the previous conclusion from the wind tunnel results.

The lift coefficient curve of a single airfoil at $Re \geq= 200,000$ remains the same with a very less increment in the maximum value, which indicates further increase in the Reynolds number and will not improve the maximum lift coefficient value. The double-element airfoil lift coefficient at $Re \geq= 200,000$ is increasing and a stall condition of an airfoil is yet to reach at 20° angle of attack. The maximum lift coefficient of a single airfoil is increased by 40% at $Re = 200,000$ and the angle of attack by 20° in the double-element airfoil. At an angle of attack below 12° the lift coefficient curves of the double-element airfoil at the $Re \geq= 200,000$ follows sagging nature in the curve, as compared to a single airfoil lift coefficient curve. It indicates that, the double-element airfoil is not having any effect of an increase in a lift coefficient under this condition. Therefore, wind tunnel results show that, the double-element airfoil is effective at $Re \geq= 100,000$ for a S1210 airfoil.

4. 2D CFD modeling and simulation

In this study, a 2D geometric mesh was created using ANSYS ICEM CFD. The domain was a circle with a radius of 4 m, corresponding to 40 times the chord length of the main airfoil. A structured Hexa mesh was used. The height of the first cell from the boundary surface was $3\mu m$, which grew at a ratio of 1.2. A smooth transition was maintained between the smaller boundary quad elements and the much larger elements away from the airfoil surfaces.

The boundary layer was captured by using the O-Grid blocking topology within ICEM CFD in a C-shaped pattern. The boundary layer around the airfoil and the wake zone with finer sized mesh elements behind the airfoil were captured with the C-shaped O-Grid. First, a grid was fixed to a distance of $1.0x10^{-6}m$ to ensure a dimensionless number $y+ \leq 1.5$, to properly resolve the boundary layer close to the wall surface and to obtain accurate reports of the lift and drag coefficient (between the domain and boundary layer). The use of a structured mesh with a circular air domain to simulate different angles of attack increased the flexibility of mesh generation and the convergence in the solution. The cell count was 150,000. Figure 7 shows the mesh used for the double-element S1210 airfoil. Air was considered to be an isothermal

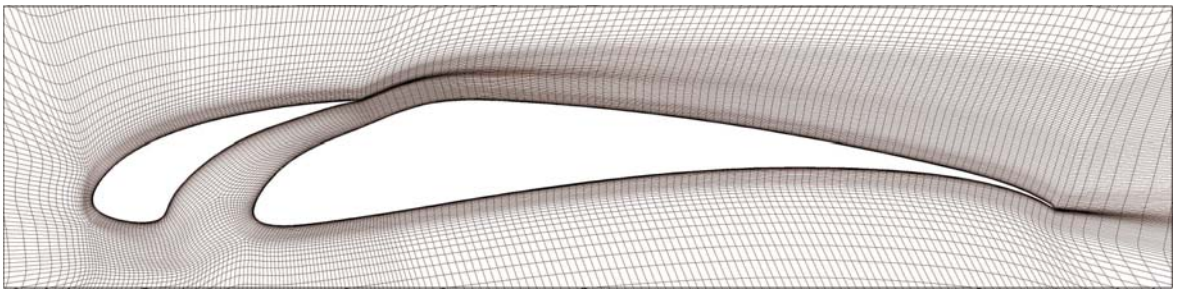

Figure 5. Grid around double-element Airfoil

and incompressible gas with constant density in the solver settings. A single set of momentum equations was solved. Mass and force balances were ensured by using the continuity equation and the momentum equation set in the solver, respectively. To simulate turbulence, the viscous Spalart All-maras (1 equation) model was used, with the Strain/Vorticity-based SA Production

mode. This mode was developed for aerospace lift and drag studies and has been used to simulate airfoils. It is a computationally efficient mode that can predict wall forces accurately and has been developed basically for aerospace lift and drag studies. On top of that, this model is chosen because it is computationally efficient and it has been used to correctly simulate airfoil.

To solve the system of governing partial differential equations, the continuity equation was discretized. The Reynolds average Navier-Stokes equation (RANS) was formulated by using a finite volume method with an algebraic segregated solver, as implemented in ANSYS Fluent. Continuity and momentum equations were linked by the Semi-Implicit Method for Pressure-Linked Equations (SIMPLE) algorithm. An algebraic multigrid (AMG) technique was used in the iterative solver to obtain improved convergence rates. All simulations were performed under steady-state conditions. Under relaxation conditions, factors of 0.2 and 0.6 were applied to the pressure and momentum parameters, respectively, trading processing speed for more accurate prediction of the physics. A run was continued until the lift and drag coefficients attained steady values that indicated a converged solution.

At the airfoil walls, the no-slip boundary condition was assumed, which is an appropriate condition for the velocity component at the wall. At the domain boundary, a velocity inlet-type boundary condition was applied, in which the free-stream velocity was set, and the angle of attack was changed between $\pm 40°$. Multiple simulations were performed at different angles of attack for $Re = 200,000$.

Figure 7 shows the lift and drag coefficients of the double-element airfoil obtained from CFD simulations and compared to the wind-tunnel results. The CFD lift coefficient curve showed a

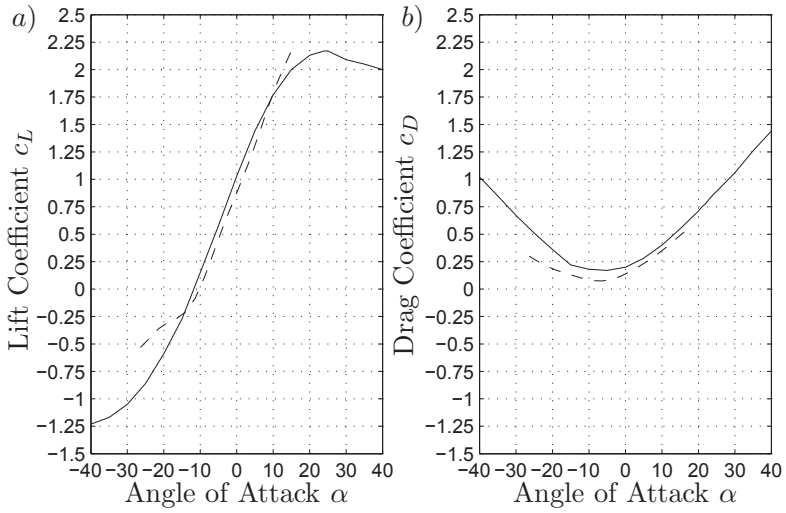

Figure 6. 2D CFD model validation for double-element S1210 airfoil at $Re = 200,000$.
a) Lift coefficient. b) Drag coefficient.
- - - - - : Wind tunnel results —— :2D CFD results

very good fit with the wind-tunnel results (Figure 7.a). At angles of attack $\alpha \geq 10°$, the lift curve in the wind-tunnel testing began to increase. The simulated lift curve from the 2D CFD model showed the real situation of the flow physics due to non-confined flow, in which the stall angle was the real stall angle of the double-element S1210 airfoil.

The value of the stall angle for the double-element S1210 airfoil was 25°, compared to 15° for the single S1210 airfoil. A large difference in stall angle between the airfoils ($\alpha_{stall} = 10°$) will contribute to increased airfoil power performance. The design proposed in this paper for

the double-element airfoil achieved a delay in the stall angle by using a slat airfoil in front of the main airfoil. The accuracy of the 2D CFD results were within 5% for an angle of attack (α) in the range of $\pm 15°$. For $\alpha \geq 10°$, the 2D CFD model underestimated the lift coefficient.

5. Conclusion

A low Reynolds number, a high lift airfoil is selected to design a double-element airfoil. A simple way of dividing a single airfoil into a double-element airfoil is given, based on the literature of double-element airfoil flow physics. It is certainly a rough estimate of slat and main airfoil sizes due to very limited or almost zero available research work on two-element airfoil for $Re \leq 500,000$ particularly used in a wind energy application. A thin airfoil S1210 was selected which performs well at low Reynolds number $Re \leq 200,000$.

A wind tunnel test for a single S1210 airfoil and a double-element S1210 airfoil has been performed for various Reynolds numbers. It is observed from the wind tunnel tests that, the use of a double-element airfoil instead of a single airfoil has increased the lift coefficient and delayed the stall angle which is very advantageous in the VAWT. An increase in the maximum lift coefficient for $Re \geq 100,000$ has been very prominent which, indicates that, at the low wind speed the double-element airfoil performance has been considerable. It is also observed that, there is decrease in the lift coefficient of a double-element airfoil under the angle of attack at which the single airfoil stalls. This phenomenon is not explainable at this stage. The wind tunnel test results are further used to validate the 2D CFD model for the double-element airfoil.

The validation of a 2D CFD model has been a critical part of this research work. A mesh quality had been ensured at the critical area between the slat and the main airfoil by refined mesh. The 2D CFD simulations are in an acceptable range. However, it will be a very accurate validation, if the 3D CFD simulation is performed. A best compromise between the expense of 3D CFD simulation and quality of 2D CFD simulation data obtained in this work was made. Finally, 2D CFD data was accepted for further research work. Further, research needs to carry out in both case wind tunnel experiment and the CFD simulation.

Acknowledgments

The SYSWIND project (project no. 238325) funded by the Marie Curie Actions is acknowledged for the financial support under the grant Seventh Framework Programme for Research and Technological Development of the EU.

References

[1] Darrieus G. J. M., 1931, Turbine having its rotating shaft transverse to the flow of the current, United States Patent office, Patent No. 1835018.
[2] Muller G., Jentsch M. F., Stoddart E., 2009, Vertical axis resistance type wind turbines for use in buildings, Renewable Energy, Vol. 34, pg. 1407-1412.
[3] Sharpe T., Proven G., 2010, Crossflex: Concept and early development of a true building integrated wind turbine, Energy and Buildings, Vol. 42, pg. 2365-2375.
[4] Eriksson S., Bernhoff H., Leijon M., 2008, Evaluation of different turbine concepts for wind power, Renewable and Sustainable Energy Reviews, Vol. 12, pg. 1419-1434.
[5] Chougule P.D., Nielsen S.R.K., 2014, Overview and Design of self-acting pitch control mechanism for vertical axis wind turbine using multi body simulation approach, A proceedings of Science of making true from wind 2014, under peer review.
[6] Bhutta M. M. A., Hayat N., Fahrooq A.U., Ali Z., Jamil Sh. R., Hussian Z., 2008, Evaluation of different turbine concepts for wind power, Renewable and Sustainable Energy Reviews, Vol. 12, pg. 1419-1434.
[7] Smith A. M. O. , 1975, Hight Lift Aerodynamics, Journal of Aircraft, Vol. 12 , N0. 6.
[8] Bah E. A., Sankar L., Jagoda J., 2013, Investigation on the Use of Multi-Element Airfoils for Improving Vertical Axis Wind Turbine Performance, 51st AIAA Aerospace Sciences Meeting Including The New Horizons Forum and Aerospace Exposition.
[9] Lew P., 2011, Multi-element wind turbine airfoils and wind turbines incorporating the same, United States Patent office, Patent no. US 2011/0255972 A1.

[10] M. Gaunaa, N. N. Sørensen and C. Bak, 2010, Thick multiple element airfoils for use on the inner part of wind turbine rotors, The science of making torque from wind, June 28-30, Crete, Greece.
[11] Buhl T., 2009, Research in Aeroelasticity EFP-2007-II, Ris-R 1698(EN).
[12] Giguere P., Selig M.S. 1997, Low Reynolds number airfoils for small horizontal axis wind turbines, Wind Engineering, Vol. 21 No. 6, pg. 367-380.
[13] Mohamed M.H., 2012, Performance investigation of H-rotor Darrieus turbine with new airfoil shapes, Energy, Vol. 47 No. 6, pg. 522-530.
[14] Claessens M. C., November 2006, The design and testing of airfoils for application in small vertical axis wind turbines, A Master Thesis, Delft University of Technology.
[15] Selig M.S. , Guglielmo J.J., Broeren P., Giguère P., 1995, Summary of Low-Speed Airfoil Data, Volume 1, SoarTech Publications, Virginia Beach, Virginia.
[16] Selig M.S. , McGranahan B.D., 2003, Wind Tunnel Aerodynamic Tests of Six Airfoils for Use on Small Wind Turbines Period of Performance, NREL/SR-500-34515, pg. 64.
[17] Singh R. K. , Ahmed M. R., Zullah M. A. , Lee Y-H. , 2012, Design of a low Reynolds number airfoil for small horizontal axis wind turbines, Renewable Energy vol. 42, pg. 66-75.
[18] Aerolab, Aerolab,Educational Wind Tunnel, Maryland USA, http://www.aerolab.com/downloadable-documents/ewtbrochure.pdf.